Functional Materials 14, No.1 (2007)

Short-range atomic order in f.c.c.–Ni–9 at.% Al solid solution

S.M.Bokoch, M.P.Kulish, V.V.Ryashko, O.V.Snagovskiy, V.A.Tatarenko*

Physics Faculty, T.Shevchenko Kyiv National University,
6 Acad. Glushkov Ave., 03022 Kyiv, Ukraine
*G.Kurdyumov Institute for Metal Physics,
National Academy of Sciences of Ukraine,
36 Acad. Vernadsky Blvd., 03680 Kyiv-142, Ukraine

The short-range atomic order for a single crystal of f.c.c.–Ni–9 at.% Al solid solution quenched from 1073 K, as well as the short-range order transformations initial stages during isothermal annealing at 373 K have been investigated using the diffuse X-ray scattering method. Specific features of the thermal two-phonon diffuse scattering have been analyzed. It is shown that in quenched state, the short-range order corresponds to the presence of concentration waves in the alloy with ordering vectors $\mathbf{k}_s = X(001)$ and $\mathbf{k}_s = (000.2)$. The initial ordering kinetics stages are accompanied by a considerable increasing of the short-range order diffuse intensities for vectors close to the structural one. The time dependence of the Warren-Cowley short-range order parameters, as well as local atomic configurations simulation results (using the Monte-Carlo technique), have shown that such transformations correspond to the nucleation and growth of the two short-range ordered regions: clustered (decomposing) and $L1_2$-type weakly ordered (Ni_3Al) ones.

Методом диффузного рассеяния рентгеновских лучей исследовано строение ближнего атомного порядка монокристаллического сплава твердого раствора замещения ГЦК–Ni–9 ат.% Al, закаленного от 1073 К, а также начальные стадии превращений ближнего порядка в процессе изотермического отжига сплава при температуре 373 К. Проанализированы особенности двухфононного теплового диффузного рассеяния. Показано, что в закаленном состоянии строение ближнего порядка соответствует присутствию в сплаве концентрационных волн с векторами упорядочения $\mathbf{k}_s = X(001)$ и $\mathbf{k}_s = (000,2)$. При этом начальные стадии кинетики упорядочения сопровождаются значительным ростом диффузной интенсивности ближнего порядка для векторов, близких к структурному. Временная зависимость параметров ближнего порядка Уоррена-Каули, а также результаты расчета локальных атомных конфигураций по методу Монте-Карло показали, что такие превращения соответствуют зарождению и росту двух ближнеупорядоченных областей: распадающейся и слабо упорядоченной по $L1_2$-типу (Ni_3Al).

The high-temperature stability of physical and mechanical properties of Ni–Al alloys has provided a major prospect of their use in engineering as multi-functional materials. A specific feature of this system is that it conserves a high degree of atomic ordering up to the melting point. Certainly, this phenomenon is conditioned by the considerable pair interaction energies of Ni and Al atoms and, as a consequence, a specific spatial distribution of alloy components (superstructure formation). So, for example, in the region enriched in Ni, at Al contents $c_{Al} \approx 25$ at.% the $L1_2$-type ordered cubic superstructure (Ni_3Al) is formed on the basis of disordered f.c.c. solid solution [1–11]. At Al contents $c_{Al} \approx 50$ at.%, the $L1_0$-type superstructure (NiAl) is formed [1]. Second, in spite of the strongly pronounced atomic order, Ni–Al system in the Al concentration region of $0 \le c_{Al} \le 25$ at.%, the magnetic

order is formed due to non zero spins of Ni atoms with temperature-dependent values [12]. Third, because of a considerable size difference of Ni and Al atoms and, as a consequence, large deformations ("strain-induced") effects, Ni–Al alloys are known to be inclined to isostructural decomposition (at Al contents $c_{Al} > 10–12$ at.%) [2–4]. Thus, a detailed studying of the ordering process and its time evolution in this system will allow to establish a correlation between microscopic and macroscopic physical characteristics of the alloy.

The qualitatively thermodynamically equilibrium spatial distribution of the components as well as the ordering kinetics can be investigated using electron microscopy and electron diffraction techniques. At the same time, the only quantitative method to study atomic correlation effects in alloys is the diffuse X-ray (or thermal neutrons) scattering. That method was used before to investigate the short-range order equilibrium states for Ni–Al solid solutions of several compositions quenched from various temperatures T_q: Ni–7.3 and 10.5 at.% Al (T_q = 673, 823 K) [8], Ni–8.9 at.% Al(T_q = 775 K) [9], Ni–9.5 and 9.8 at.% Al (T_q = 973 K) [7], Ni–12.7 at.% Al (T_q = 1323 K) [6] and alloys Ni–46.2; 50,04; 58.2 at.% Al (T_q = 1473 K) [5]. Basing on those studies, the Warren-Cowley short-range order parameters, Fourier components (and originals) for static and dynamic local lattice distortions [10] and the total "mixing" energies were determined. Basing on obtained results, was established that short-range atomic order in Ni–Al solid solutions belongs to $L1_2$-type (Ni_3Al). At the same time, electron-microscopic studies of other authors [3] and [2, 4] testify to the presence of decomposition processes in alloys with the specified Al contents. A more reliable establishing of ordering and/or clustering processes in Ni–Al system is possible only by studying the time dependences of interatomic correlation parameters at early relaxation stages, as it is made in this work using the diffuse X-ray scattering kinetics.

To research the interatomic correlations in Ni–Al alloys, the Ni–9 at.% Al solid solution single crystal was chosen. The single crystal of 2×8×10 mm^3 size was grown in an alundum crucible with a conic seed part in argon atmosphere. An outer facet of the sample was cut parallel to the (001) plane. The initial state has been obtained by quenching from T_q = 1073 K of a sample previously annealed during 8 hours. The quenching was carried out in 10 wt.% aqueous NaOH (at room temperature) in a special device. Then the sample was annealed isothermally at T_a = 373 K. The X-ray diffuse scattering was measured using MoK_α radiation (using a DRON-3 unit at U = 32 kV and I = 32 mA). Such regime provided separation of hard radiation high harmonics $\lambda/2$, $\lambda/3$, etc., and the fluorescence component from the spectrum of beam monochromated previously by a LiF crystal monochromator [13]. To transform the diffuse intensity into absolute electron units, the scattering intensity from low-absorbing fused quartz [14] was used as a reference. The correction for absorption was taken into account, too, in case of inclined diffraction geometry of the sample examination [14].

The components caused by the Laue background modulation (short-range order, static and dynamic local lattice distortions, etc.) were separated using the Cohen-Georgopoulos separation techniques [15–17]. The separation is based on the symmetry differences of the diffuse background modulation functions by scattering components in the reciprocal space. So, in general, the diffuse scattering intensity, according to [11], can be presented as

$$I_{\text{Diff}}(\mathbf{k}) = Nc_Ac_B(f_A - f_B)^2 \times \left[I_{\text{SRO}}(\mathbf{k}) + I_{\text{ST.D}}(\mathbf{k}) + I_{\text{DYN.D}}(\mathbf{k})\right] + I^2_{\text{TDS}}(\mathbf{k}) + I^{3+4+\cdots}_{\text{TDS}}(\mathbf{k}) + I_{\text{Comp}}(\mathbf{k}),$$

where term $Nc_Ac_B(f_A - f_B)^2$ defines the so-called Laue multiplier (N is the number of atoms in the unit cell; c_A, c_B, f_A, f_B, atomic concentrations of the alloy components and their scattering factors, respectively); that term defines the diffuse background intensity for the alloy at 0 K, at absence of interatomic correlations and zero static and dynamic distortions of first and higher orders. $I_{\text{SRO}}(\mathbf{k})$, $I_{\text{TDS}}{}^2(\mathbf{k})$, $I_{\text{TDS}}{}^{3+4+\cdots}(\mathbf{k})$ are the intensities caused by the interatomic correlations, thermal two-phonon and multiphonon diffuse scattering, respectively. $I_{\text{Comp}}(\mathbf{k})$ is the Compton scattering intensity. $I_{\text{ST.D}}(\mathbf{k})$, $I_{\text{DYN.D}}(\mathbf{k})$ is the Fourier components of the static and dynamic crystal lattice local distortions defined by relations [11]:

$$I_{\text{ST.D}}(\mathbf{k}) = \sum_{i=x,y,z} h_i[\eta Q_i^{\text{AA}}(\mathbf{k}) + \xi Q_i^{\text{BB}}(\mathbf{k})],$$

$$I_{\mathrm{DYN.D}}(\mathbf{k}) =$$

$$= \sum_{i=x,y,z}(h_i)^2[\tilde{\eta}^2 R_i^{\mathrm{AA}}(\mathbf{k}) + 2\tilde{\eta}\tilde{\xi}R_i^{\mathrm{AB}}(\mathbf{k}) + \tilde{\xi}^2 R_i^{\mathrm{BB}}(\mathbf{k})] +$$

$$+ \sum_{i>j}\sum_{j} h_i h_j[\tilde{\eta}^2 S_{ij}^{\mathrm{AA}}(\mathbf{k}) + 2\tilde{\eta}\tilde{\xi}S_{ij}^{\mathrm{AB}}(\mathbf{k}) + \tilde{\xi}^2 S_{ij}^{\mathrm{BB}}(\mathbf{k})],$$

where $\mathbf{k} = \mathbf{i}h_x + \mathbf{j}h_y + \mathbf{k}h_z$, $\eta = \mathrm{Re}f_{\mathrm{A}}/(f_{\mathrm{A}} - f_{\mathrm{B}})$, $\xi = \mathrm{Re}f_{\mathrm{B}}/(f_{\mathrm{A}} - f_{\mathrm{B}})$, $\tilde{\eta}^2 = |f_{\mathrm{A}}|^2/|f_{\mathrm{A}} - f_{\mathrm{B}}|^2$, $\tilde{\xi}^2 = |f_{\mathrm{B}}|^2/|f_{\mathrm{A}} - f_{\mathrm{B}}|^2$, $\tilde{\eta}\tilde{\xi} = \mathrm{Re}f_{\mathrm{A}}f_{\mathrm{B}}/|f_{\mathrm{A}} - f_{\mathrm{B}}|^2$, Here, $Q_i^{\mathrm{AA(BB)}}(\mathbf{k})$, $R_i^{\mathrm{AA(AB)(BB)}}(\mathbf{k})$, $S_{ij}^{\mathrm{AA(AB)(BB)}}(\mathbf{k})$ are projections of the Fourier components onto the reciprocal lattice axes ($i = x,y,z$) of linear static, quadratic static and dynamic atomic displacements, including the Xuang scattering and the single-phonon diffuse one. The all presented components are related to their Fourier originals in the direct space by the relationships:

$$I_{\mathrm{SRO}}(\mathbf{k}) = \sum_{lmn}\alpha_{lmn}\cos(\pi h_x l)\cos(\pi h_y m)\cos(\pi h_z n),$$

$$Q_x^{\mathrm{AA}}(\mathbf{k}) = -2\pi\sum_{lmn}(c_{\mathrm{A}}/c_{\mathrm{B}} + \alpha_{lmn}) < x_{lmn}^{\mathrm{AA}} > \times$$
$$\times \sin(\pi h_x l)\cos(\pi h_y m)\cos(\pi h_z n)\},$$

$$Q_x^{\mathrm{BB}}(\mathbf{k}) = 2\pi\sum_{lmn}\{(c_{\mathrm{B}}/c_{\mathrm{A}} + \alpha_{lmn}) < x_{lmn}^{\mathrm{BB}} > \times$$
$$\times \sin(\pi h_x l)\cos(\pi h_y m)\cos(\pi h_z n)\},$$

$$R_x^{\mathrm{AA}}(\mathbf{k}) = -2\pi^2\sum_{lmn}(c_{\mathrm{A}}/c_{\mathrm{B}} + \alpha_{lmn}) \times$$
$$\times < x_{000}^{\mathrm{A}} x_{lmn}^{\mathrm{A}} > \cos(\pi h_x l)\cos(\pi h_y m)\cos(\pi h_z n),$$

$$S_{xy}^{\mathrm{AA}}(\mathbf{k}) = 4\pi^2\sum_{lmn}\{(c_{\mathrm{A}}/c_{\mathrm{B}} + \alpha_{lmn}) \times$$
$$\times < x_{000}^{\mathrm{A}} y_{lmn}^{\mathrm{A}} > \sin(\pi h_x l)\sin(\pi h_y m)\sin(\pi h_z n)\}.$$

In this case, the $Q_x^{\mu\mu}(h_x,h_y,h_z) = Q_y^{\mu\mu}(h_y,h_z,h_x) = Q_z^{\mu\mu}(h_z,h_x,h_y)$ are valid. Such type symmetry in the reciprocal space is inherent in $R_i^{\mu\nu}$ $(\mathbf{k})$ and $S_{ij}^{\mu\nu}(\mathbf{k})$ scattering components (μ, ν = A, B). Using the reverse Fourier transformation of the specified Fourier components, their values in direct space can be determined. So, for example, the quantity α_{lmn} means deviation of the two-particular probability (finding of B(A)-type atom on the distance $\mathbf{r}(lmn)$ to A(B)-type atom) ratio to the average atomic concentration of the same B(A)-type atoms in the crystal from 1. In general case, the number of all scattering components modulating the Laue background is 25. For their correct separation, it is necessary to measure the diffuse scattering intensities in 25 equivalent volumes of the reciprocal space.

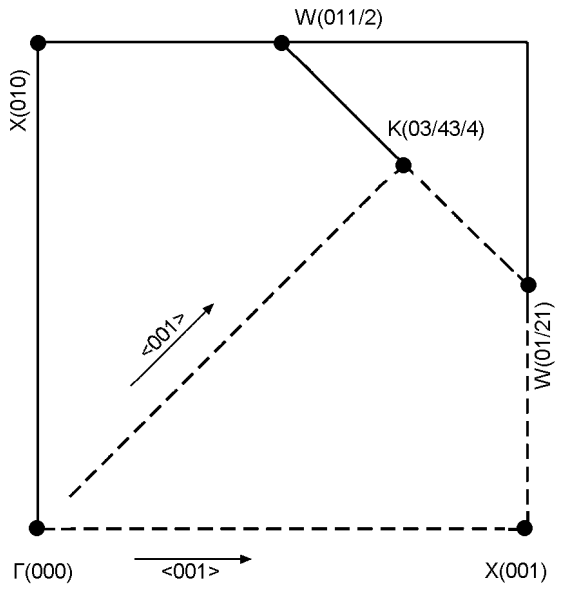

Fig. 1. High symmetry points (•) and first irreducible f.c.c.-lattice Brillouin zone (- - -) where diffuse scattering intensities $I_{\mathrm{SRO}}(\mathbf{k})$ from Ni–9 at.% Al solid solution were measured. The $(001)^*$ plane is shown.

Taking into account the transformation features in Ni–Al alloys, our measurements were carried out in the superstructural points $\mathbf{k} = X[2\pi/a(001)]$, $W[2\pi/a(01/21)]$, (short-range ordering regions) and close to the structural (fundamental) ones $\mathbf{k} \to \Gamma[2\pi/a(000)]$ (clustering regions) points, and in directions such as <100> and <110> pertinent of the wave vectors regions of first irreducible f.c.c.-lattice Brillouin zone (Fig. 1).

It is known that, when studying the diffuse background in alloys caused by the interatomic correlation effects, it is necessary to take into account correctly the parasitic components caused by scattering on the lattice thermal vibrations-two-phonon $I_{\mathrm{TDS}}^2(\mathbf{k})$ and multi-phonon scattering $I_{\mathrm{TDS}}^{3+4+\cdots}(\mathbf{k})$. These scattering components have been calculated theoretically. According to the theory presented in [18,19], the two-phonon and multi-phonon scattering intensity is defined as:

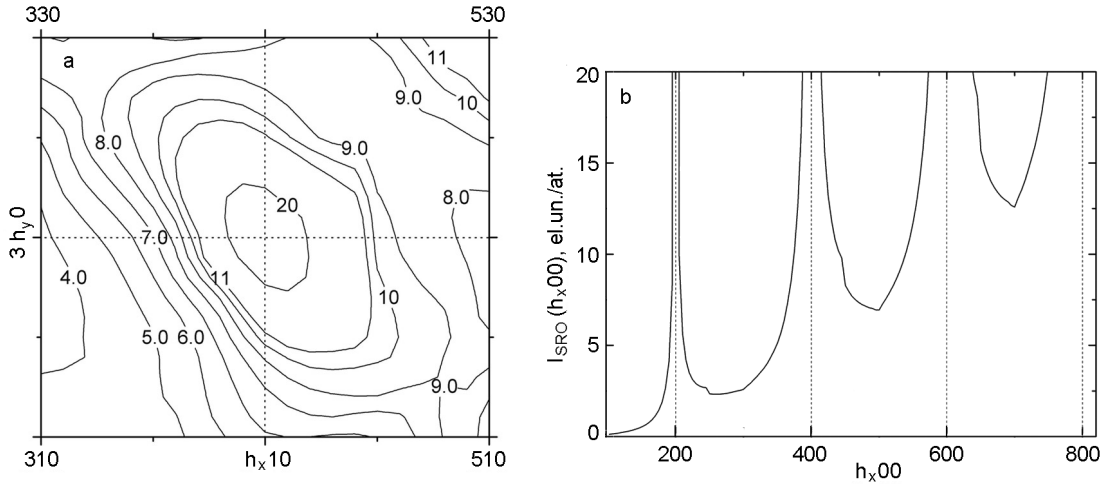

Fig. 2. Two-phonon diffuse scattering intensities distributions, $\{(I^2_{TDS}(\mathbf{k})$, near the structural (fundamental) reflex (420) (a) and its dispersion dependence along the <100> direction (b). Intensities are presented in electron units per atom.

$$I^2_{\mathrm{TDS}}(\mathbf{k}) = \frac{f^2\exp(-2M)}{2m}\upsilon_0|\mathbf{k}|^4 \times$$

$$\times \sum_{h_x h_y h_z} \int \sum_{i,j=1,2} \frac{E_{qi}E_{q'j}}{\nu^2_{qi}\nu^2_{q'j}}\cos(\mathbf{k},U_{qi})\cos^2(\mathbf{k},U_{q'j})dV,$$

$$I^{3+4+\cdots}_{\mathrm{TDS}}(\mathbf{k}) =$$

$$= Nf^2[1 - \exp(-2M)(1 + 2M + M^2)],$$

where M is the Debye-Waller factor; U_{qi}, $U_{q'j}$, polarization vectors of the thermal vibration modes; E_{ql}, $E_{q'l}$, ν_{qi}, $\nu_{q'j}$ energies and frequencies for interacting phonons.

In Fig. 2, the calculated values of the thermal two-phonon diffuse scattering intensities $I^2_{\mathrm{TDS}}(\mathbf{k})$ for Ni–9 at.% Al alloy (at T = 300 K) are shown.

The two-phonon scattering intensity is seen to increase considerably near to the fundamental Bragg reflexes ($\mathbf{k} \to \Gamma(000)$ though it cannot be neglected in superstructural positions, too.

Using the above theory, the X-ray diffuse scattering intensity components have been separated for a single crystal sample of Ni–9 at.% Al solid solution quenched from 1073 K and isothermally annealed at temperature 373 K. In Fig. 3, shown are the isodiffuse scattering intensity distribution and kinetic dependences of the intensity caused by interatomic correlations, $I_{\mathrm{SRO}}(\mathbf{k})$, and also Warren-Cowley short-range order parameters $\alpha(\mathbf{r}_n)$ ($\mathbf{r}_n$ is radius-vector for n-th co-ordination shell) for the sample quenched and annealed during 15 min.

It is seen from Fig. 3a that the diffuse intensity $I_{\mathrm{SRO}}(\mathbf{k})$ is concentrated mainly in high symmetry superstructural points $X(010)$ of the Brillouin zone as well as near to the structural reflexes $\Gamma(000)$. It is to note that in quenched state, the diffuse intensity in X points is 2.5 Laue units while in the (000.2) ($\mathbf{k} \to \Gamma$) positions, this value is 27 Laue units. Thus, the short-range atomic order in Ni–9 at.% Al alloy can be related preferentially to that corresponding to the short-range clustering (or decomposition) in a weakly ordered $L1_2$ type matrix. Such conclusion can be drawn also from the kinetic dependences of Warren-Cowley short-range order parameters $\alpha(\mathbf{r}_n,t)$ (Fig. 3b) which are positive up to the third co-ordination shell and increases with the annealing duration. Also, it is seen from the diffuse intensity time profiles (Fig. 3c) that at initial $I_{\mathrm{SRO}}(\mathbf{k} = X)$ relaxation stages, the intensity remains essentially constant, in contrast to $I_{\mathrm{SRO}}(\mathbf{k} \to \Gamma$ increasing noticeably in time. It is to pay attention to the lattice parameter dependence on the annealing duration $a(t)$ (Fig. 3d) which decreases during the annealing, thus confirming the development of the short-range clustering. All presents kinetic dependences specify that the short-range clustering process in Ni–9 at.% Al alloy can be related to spinodal decomposition (formation of the two short-range ordered regions with different compositions after quenching).

Taking into account the complexity of the short-range order transformations in Ni–Al alloys, the simulation of local atomic configurations must be of interest. In our case, computer simulations of the short-range order in Ni–9 at.% Al solid solution

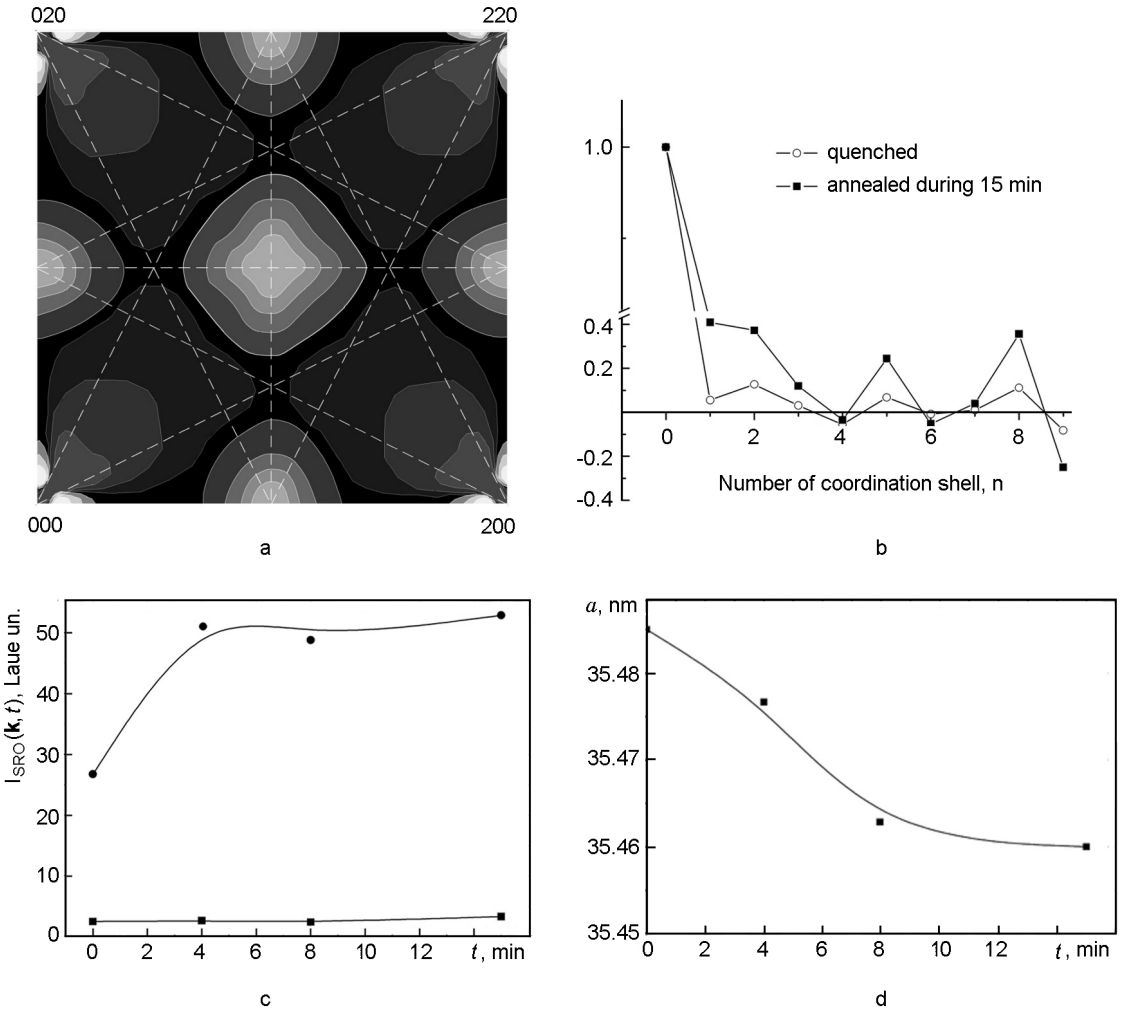

Fig. 3. Short-range order diffuse intensity distribution, $I_{SRO}(h_x h_y h_z)$, for the quenched sample (a) and Warren-Cowley parameters $\alpha(\mathbf{r}_n)$ for two states: quenched and annealed during 15 min at 373 K (b). Kinetic intensity dependences $I_{SRO}(\mathbf{k},t)$ for wave vectors $\mathbf{k} = X(2\pi/a[010])$ — ■ and $\mathbf{k} \to \Gamma(2\pi)/a[000])$ — • (c), and the lattice parameter time dependence $a(t)$ (d).

has been carried out by Monte Carlo method developed in [20–26], using the experimentally obtained Warren-Cowley short-range order parameters $\alpha(r_{lmn})$. The cyclic boundary conditions were applied to the modeling crystallite. The simulations was carried out for a three-dimensional f.c.c.-lattice array with 216,000 atomic positions. For the alloy with 9 at.% Al, this array contained 19,440 atomic positions for alloying Al atoms. Initially, the random atomic distribution (Fig. 4a) was generated. It is seen that for such distribution, there are no specific features in local atomic spatial correlations. Then, Ni and Al atoms (randomly selected) exchanged their positions, and then the following parameter was calculated:

$$R = \frac{\sum_{lmn} (\alpha_{lmn}^{calc} - \alpha_{lmn}^{exp})^2}{\sum_{lmn} (\alpha_{lmn}^{exp})^2},$$

where α_{lmn}^{exp}, α_{lmn}^{calc} are experimental and calculated Warren-Cowley short-range order parameters (after each of the atomic exchange), respectively. If the R value decreased, both kinds of atoms remained in their new positions. Otherwise, they were returned to the initial positions. In the simulations, we were limited R to the value ~10^{-6}. Fig. 4b shows the atomic distribution for the short-range ordered state of Ni–

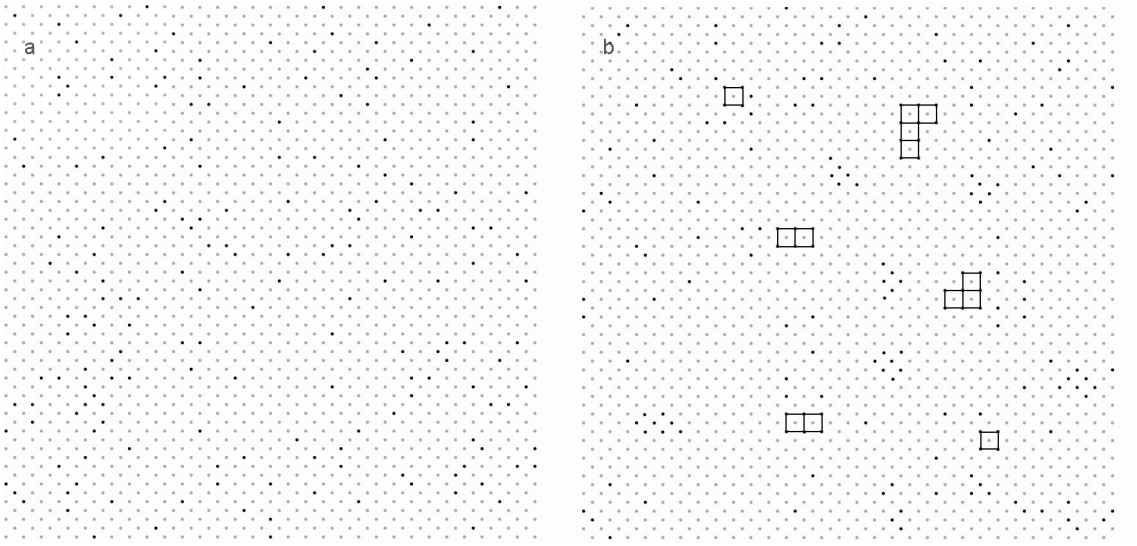

Fig. 4. The short-range order computer simulations in Ni–9 at.% Al alloy by the Monte Carlo method: random atomic distribution (a), after quenching from 1073 K and the subsequent annealing at 373 K during 15 min (b).

9 at.% Al alloy quenched from 1073 K and then annealed at 373 K during 15 min.

It is seen from Fig. 4b that in alloy after isothermal annealing during 15 min, there is a slight number of the ordered $L1_2$ type clusters (Ni_3Al), and also the short-range clustering regions. The simulation of the short-range order in Ni–9 at.% Al solid solution confirms the presence of several concentration waves with various wave ordering vectors $\mathbf{k}_s$ in the alloy.

To conclude, using the measurements of X-ray diffuse scattering intensity kinetics, the initial stages of short-range clustering (decomposition) and short-range ordering in the single crystal f.c.c.–Ni–9 at.% Al solid solution has been studied. It is shown that diffuse scattering intensity is concentrated mainly around two ordering wave vectors $\mathbf{k}_s = X(2\pi/a[010])$ and $\mathbf{k}_s \to \Gamma(2\pi/a[000])$, corresponding to the two concentration waves. The relaxation process kinetics during isothermal annealing is characterized by an insignificant increase of diffuse intensity $I_{SRO}(\mathbf{k},t)$ in superstructural points X and by a sharp increase in positions close to the Γ points. The time dependence of the Warren-Cowley short-range order parameters $\alpha(\mathbf{r}_n,t)$, as well as the local order configurations simulations (by the Monte Carlo method) have shown that the spatial redistribution of alloy components corresponds to nucleation and growth of the two short-range ordered regions: clustered and $L1_2$ type weakly ordered (Ni_3Al).

References

1. H.Y.Geng, M.H.F.Sluiter, N.X.Chen, *Phys. Rev. B.*, **72**, 014204 (2005).
2. W.O.Centry, M.E.Fine, *Acta Metall.*, **20**, 181 (1972).
3. C.L.Corey, B.Z.Rosenblum, G.M.Greene, *Acta Metall. (Mater.)*, **21**, 837 (1973).
4. W.A.Soffa, D.E.Laughlin, *Acta Metall.*, **37**, 3019 (1989).
5. P.Georgopoulos, J.B.Cohen, *Acta Metall. (Mater.)*, **29**, 1535 (1981).
6. J.E.Epperson, P.Furnrohr, *Acta Cryst.(A)*, **39**, 740 (1983).
7. F.Klaiber, B.Schonfeld, G.Kostorz, *Acta Cryst. (A)*, **43**, 525 (1987).
8. F.Chassagne, M.Bessiere, Y.Calvayrac et al., *Acta Metall. (Mater.)*, **37**, 2329 (1989).
9. B.Schonfeld, L.Reinhard, G.Kostorz, W.Buhrer, *Acta Metall. (Mater.)*, **45**, 5187 (1997).
10. B.Schonfeld, G.Kostorz, M.Celino, V.Rosato, *Europhys. Lett.*, **54**, 482 (2001).
11. B.Schonfeld, *Prog. Mater. Sci.*, **44**, 435 (1999).
12. V.A.Tatarenko, V.V.Odnosum, Yu.N.Koval', G.E.Monastyrskiy, *Metallofiz. Noveishie Tekhnol.*, **25**, 1111 (2003).
13. N.P.Kulish, N.A.Melnikova, P.V.Petrenko et al., *Izv. Vuzov. Fizika*, No.2, 82 (1989).
14. V.G.Poroshin, N.P.Kulish, *Metallofiz. Noveishie Tekhnol.*, **21**, 75 (1999).
15. P.Georgopoulos, J.B.Cohen, *J. de Phys.(C) (Paris)*, **38**, 7191 (1977).
16. P.Georgopoulos, J.B.Cohen, *Acta. Mater. (Metall.)*, **29**, 1535 (1981).
17. J.B.Cohen, *Solid State Phys.*, **39**, 131 (1986).
18. C.B.Walker, *Phys. Rev.*, **103**, 547 (1956).

19. R.Colella, B.W.Batterman, *Phys. Rev. B.*, **1**, 3913 (1970).
20. X.-M.Zhu, H.Zabel, *Acta Cryst. (A)*, **46**, 86 (1990).
21. S.H.Rahman, *Acta Crystr. (A)*, **49**, 68 (1993).
22. S.H.Rahman, *Acta Cryst. (A)*, **49**, 56 (1993).
23. S.H.Rahman, M.Rodewald, *Acta Cryst. (A)*, **51**, 153 (1995).
24. K.Osaka, T.Takama, *Acta Mater. (Metall.)*, **50**, 1289 (2002).
25. S.Hata, T.Mitate, N.Kuwano et al., *Mater. Sci. Eng. (A)*, **312**, 160 (2001).
26. S.M.Bokoch, N.P.Kulish, T.D.Shatniy, *Metallofiz. Noveishie Tekhnol.*, **26**, 627 (2004).

Близький порядок у твердому розчині заміщення ГЦК–Ni–9 ат.% Al

С.М.Бокоч, М.П.Куліш, В.В.Ряшко, О.В.Снаговський, В.А.Татаренко

Методом дифузного розсіяння рентгенівських променів досліджено будову близького порядку монокристалічного сплаву твердого розчину заміщення ГЦК–Ni–9 ат.% Al, загартованого від 1073 К, а також початкові стадії перетворень близького порядку у процесі ізотермічного відпалу сплаву при температурі 373 К. Проаналізовано особливості двофононного теплового дифузного розсіяння. Показано, що у загартованому стані будова близького порядку відповідає присутності у сплаві концентраційних хвиль з векторами упорядкування $\mathbf{k}_s = X(001)$ та $\mathbf{k}_s = (000,2)$. При цьому початкові стадії кінетики упорядкування супроводжуються значним зростанням дифузної інтенсивності близького порядку для векторів, близьких до структурного. Часова залежність параметрів близького порядку Уоррена-Каулі, а також результати розрахунку локальних атомних конфігурацій за методом Монте-Карло показали, що такі перетворення відповідають виникненню та росту двох близькоупорядкованих областей: такої, що розпадається (розшаровується), та слабо упорядкованої за $L1_2$-типом (Ni_3Al).